# Journal of Materials Chemistry B

Accepted Manuscript






ROYAL SOCIETY OF CHEMISTRY

www.rsc.org/materialsB

Journal Name

RSCPublishing

ARTICLE

# Engineering three-dimensional structures using bio-inspired dopamine and strontium on titanium for biomedical application

Cite this: DOI: 10.1039/xoxxoooooox

Received ooth January 2012,
Accepted ooth January 2012

DOI: 10.1039/xoxxoooooox

www.rsc.org/

Yen-Ting Liu[a], Kuan-Chen Kung[b], Chyun-Yu Yang[c], Tzer-Min Lee[b]†, Truan-Sheng Lui[a]

The excellent mechanical properties and chemical stability of titanium and its alloys have led to their wide use as a material for dental and orthopaedic implants. However, the bio-inert nature of these materials must be overcome to enhance cell affinity and cell function following implantation. Effective implants require strong interfacial bonding, mechanical stability, osteoblast attachment, enhanced spreading and growth during early stages, and induced differentiation and mineralization in later stages. This study developed an organic-inorganic multilayer coating process for the modification of titanium implants in order to improve cell responses. A three-dimensional structure comprising strontium and micro-arc oxidized (MAO) titanium was covered with a film of poly(dopamine) to form a multilayer coating. The titanium surface formed a uniform hydrophilic oxide coating, which was firmly adhered to the surface. The poly(dopamine) film facilitated the initial attachment and proliferation of cells. Cell differentiation was enhanced by the release of strontium from the coatings. Our results demonstrate the efficacy of the proposed coating process in enhancing the multi-biological function of implant surfaces.

## 1. Introduction

Titanium and its alloys have been widely used as a framework material in dental and orthopedic implants, due to their excellent mechanical properties and chemical stability. However, the natural oxide thin film which forms on titanium is bio-inert, which makes it difficult to achieve a chemical bond with living tissue.[1] The effectiveness of an implant depends on the development of strong anchorage between the material comprising the implant and existing bone tissue. Various forms of surface modification have been used to accelerate the initial osseointegration immediately after implantation in order to enhance the reactivity of the tissue and thereby shorten the healing period of the bone. Considerable research has been devoted to the development of techniques for coating titanium, such as plasma spraying,[2] electro-deposition,[3] and sputtering.[4] Currently, titanium and its alloys are commonly coated with hydroxyapatite (HA) through plasma-spraying; however surface coverage is low and a lack of uniformity in the coating hinders adhesion to the substrate.[5]

Ideally, implant surface coatings should mimic the morphology and function of natural bone in order to optimize the integration of the implant and existing human bone tissue. Porous coatings provide more surface area; therefore, microporous coatings appear to be a promising approach to the further development of dental and orthopedic implants. Micro-arc oxidation (MAO) (also commonly called "plasma electrolytic oxidation (PEO)", "microplasma oxidation (MPO)" and "spark anodizing") is an effective technique used to produce ceramic-like coatings with porous structures. Three-dimensional structures with numerous craters can improve surface properties, such as wear and corrosion resistance, as well as enhance biological performance. The dense, strongly adherent coating produced by MAO can minimize spalling and reduce osteolysis, which is generally triggered by the loosening of particles on implants. Rough surfaces can also improve early fixation and long-term mechanical stability.[6, 7] The bioactivity of MAO coatings can be further modified by combining MAO with other activation methods, such as electric polarization and ultraviolet (UV) irradiation.[8, 9] The MAO method makes it possible to incorporate multiple ions within an oxide layer, simply by adjusting the compositions of the electrolyte solutions. It has even been proposed that the introducing of Ag into an MAO coating could provide antibacterial properties.[10] In a previous study, we investigated the incorporation of manganese ions

into MAO coatings, the subsequent release of which enhanced cell differentiation and mineralization.[11]

Strontium (Sr) has been attracting considerable attention for the clinical treatment of osteoporosis. Like calcium (Ca), Sr is a bone-seeking element and approximately 98% of the total Sr in the body is localized in bone tissue. Strontium-substituted hydroxyapatite (Sr-HA) has the same charge as calcium, and has therefore been adopted as a filler material to improve the biocompatibility of bone cement.[12, 13] The presence of Sr in coatings can enhance osteoblast activity and differentiation, while inhibiting the production and proliferation of osteoclast.[14, 15] Previous studies have demonstrated the efficacy of MAO coatings incorporating strontium, calcium, and phosphate (P) in enhancing cell responses.[16]

Considerable improvements have been made in modifying the topography of implants; therefore, it is expected that the immobilization of bioactive molecules (biochemical modification) will be the next major focus. A number of naturally occurring adhesives have recently attracted attention. For example, the 3,4-dihydroxyphenethylamine (dopamine) molecule is an adhesive protein that allows mussels to adhere to a variety of materials.[17] Poly(dopamine)-based film could be used in biomedical applications as an intermediate layer for the immobilization of other biofunctional molecules.[18-20] In a previous study, we were inspired by the mussels of genus *Mytulis* to develop a synthetic adhesive platform for tissue-implant applications.[21] In the current study, we proceeded on the assumption that a poly(dopamine) film could provide a bioreactive surface with which to enhance the cell response to MAO coatings.

In the present study, the MAO method was employed to modify a titanium surface in aqueous electrolytes, such that Ca, P, and Sr could be incorporated into the porous oxide coating to improve the differentiation of osteoblast cells. We then employed self-polymerization to generate a bioactive film of poly(dopamine) on the surface of the resulting coating. The addition of dopamine and Sr was shown to alter the local chemistry and in so doing change the biological properties of the MAO coating. The result is an increase in cell response, capable of altering cell morphology, cell proliferation, and bone-related gene expression.

## 2. Materials and methods

### 2.1 Preparation of specimens

Medical grade titanium (commercially pure titanium, Grade 2, ASTM F-67 S-Tech Co., Taiwan) was used as a substrate. Substrate discs 12.7 mm (diameter) × 2 mm (thickness) were ground and polished using 1500-grit followed by ultrasonic cleaning in acetone, ethanol, and distilled water prior to MAO processing. The MAO reaction apparatus was constructed in a two-electrode electrochemical cell with DC power supply (GPS-60H15S, Good Will Instrument Co., Taiwan) using stainless steel as the cathode and the titanium specimen as the anode. The electrolyte was prepared by dissolving sodium phosphate monobasic monohydrate ($NaH_2PO_4 \cdot H_2O$, 99.7%, J.T. Baker, USA), calcium acetate hydrate ($Ca(CH_3COO)_2 \cdot H_2O$, 99%, Acros, USA) and strontium acetate hemihydrate ($Sr(CH_3COO)_2 \cdot 0.5H_2O$, 98%, Alfa Aesar, USA) in distilled water. The compositions of the electrolyte solutions are presented in Table 1. The samples were treated with an applied voltage of 350 V for 1 min with the temperature maintained at 25°C by circulating water through the electrochemical cell. As shown in Table 1, the MAO specimens are denoted as CaP and SrCaP, in accordance with the preparation of the materials in the electrolytic solution. As-prepared specimens were ultrasonically cleaned in acetone, ethanol, and distilled water prior to dopamine modification. The as-prepared specimens then underwent dopamine polymerization involving immersion in a solution of 10 mM Tris-HCl solution adjusted to pH 8.5 with added dopamine at a concentration of 2 mg/ml. The colour of the solution changed from clear to dark brown resulting from pH-induced oxidative reaction. The reaction was performed at room temperature, under mixing at 300 rpm for 12 h. The CaP and SrCaP specimens were also immersed in Tris-HCl solution to act as a control group with the same ion concentration as the test samples. All of the specimens were then rinsed using deionized water and dried with $N_2$ gas. The two resulting MAO substrates with poly(dopamine) coating were denoted as CaPD and SrCaPD, respectively. All of the specimens were sterilized using 70% ethanol and then divided evenly into a 24-well plate for cell assays.

### 2.2 Characterization of poly(dopamine) film coated on MAO coatings

The surface morphology of the specimens was observed using a scanning electron microscope (SEM, JSM-6390LV, JEOL) equipped with an energy- dispersive X-ray spectrometer (EDX, INCA/350, Oxford) for chemical analysis. The surface wettability of the specimens was determined using measurements of static contact angle. We employed the sessile drop method using a 5 μl drop of double-distilled water as probing liquid.

The surface chemistry was analysed using X-ray photoelectron spectroscopy (XPS, Thermo K-Alpha, Thermo Scientific, USA), recorded using a monochromatic Al Kα source (1486.6 eV). The photoelectron take-off angle was 45° and survey spectra were collected over a range of 0-1200 eV. The C 1s spectra was set to 284.6 eV as a reference to calibrate the scale of binding energy. Intensity ratios were converted into atomic concentration ratios using sensitivity factors.

**Table 1** Composition of the Sr-MAO electrolyte and DOPA solutions

| Specimen | Solution composition (M) | | | Sr/(Sr+Ca) | DOPA (mg/mL) |
|---|---|---|---|---|---|
| | $NaH_2PO_4 \cdot H_2O$ | $Ca(CH_3COO)_2 \cdot H_2O$ | $Sr(CH_3COO)_2 \bullet 0.5H_2O$ | | |
| Ti | -- | -- | -- | -- | -- |
| TiD | -- | -- | -- | -- | 2 |
| CaP | 0.06 | 0.13 | 0 | 0 | -- |
| CaPD | 0.06 | 0.13 | 0 | 0 | 2 |
| SrCaP | 0.06 | 0.1170 | 0.0130 | 10 | -- |
| SrCaPD | 0.06 | 0.1170 | 0.0130 | 10 | 2 |

### 2.3 Cell culture

Osteoblastic cells (MC3T3-E1, ATCC number: CRL 2593™) were obtained from the American Type Culture Collection (ATCC, USA) and maintained in alpha Minimum Essential Medium (alpha MEM, Gibco Invitrogen, USA) supplemented with 10% heat-inactivated fetal bovine serum (FBS, Gibco Invitrogen, USA), antibiotics (100 U/ml penicillin, 0.1 mg/ml streptomycin, and 0.25 μg/ml amphotericin B, Cashmere Biotech, Taiwan) at 37°C in a humidified atmosphere of 5% $CO_2$ in air. The medium was replaced twice weekly and cultured until confluence. The cells were washed twice with phosphate-buffered saline (PBS), detached using 0.05% trypsin-EDTA (Gibco Invitrogen, USA), and then centrifuged at 1000 rpm for 5 min.

### 2.4 Initial cell spreading and cytoskeleton development

The specimens were seeded with cells at a density of $3.5 \times 10^3$ cells/cm$^2$. A fluorescence microscope (Axio Observer Z1, Zeiss, Germany) and image analyser (Axio Vision, Zeiss, Germany) were used to examine cell morphology and cytoskeletal arrangement. After culturing for 3 h, cells were fixed using 4% paraformaldehyde (Sigma, USA) for 30 min and permeabilized with 0.1% Triton-X-100 (JT Baker, USA) for 15 min. After being washed with PBS, the cells were incubated in 2% BSA for 40 min. Vinculin (1:150) was labeled with monoclonal antibodies (V9131, Sigma, USA) and anti-mouse IgG conjugated with Alexa flour 594 (A11005, Molecular Probes, USA). F-actin (1:200) was stained with Alexa flour 488-labled phallodin (A12379, Molecular Probes, USA). Finally, the coverslips were incubated with DAPI (4',6-Diamidino-2-phenylindole dihydrochloride) nuclear dye and mounted in ProLong® Gold antifade reagents (Molecular Probes, USA) for analysis using a fluorescence microscope.

### 2.5 Cell proliferation

Cell suspensions of all specimens were seeded at a cell density of $5 \times 10^3$ cells/cm$^2$. Following 1, 3, and 7 days of culturing, the number of cells was determined using a 3-[4,5-dimethylthiazol-2-yl]- 2,5-diphenyltetrazolium bromide assay (MTT, Sigma, USA). For this assay, 100 μl of MTT working solution was added to each well. The MTT working solution was then removed after an incubation period of 4 h and combined with insoluble formazan crystal dissolved in dimethyl sulfoxide (DMSO). Analysis was performed using an enzyme-linked immunosorbent assay (ELISA) plate reader (Sunrise, Austria) at 570 nm. The $OD_{570}$ were plotted against a series of known cell numbers ($10^3$, $5 \times 10^3$, $10^4$, $5 \times 10^4$, $10^5$, $5 \times 10^5$ cell/well) to establish a standard calibration curve.

### 2.6 ALP activity

All specimens were seeded with cell suspensions in 24-well plates at a cell density of $5 \times 10^3$ cells/cm$^2$. After 7 days of culturing, ALP activity was measured colorimetrically using SIGMAFAST™ p-Nitrophenyl phosphate (p-NPP) tablets (Sigma, USA). 100μl p-NPP working solution was added to the supernatant and the reaction was stopped using 0.05M NaOH following incubation for 30 min at 37 °C. Analysis was performed using an ELISA plate reader (Sunrise, Austria) at 405 nm. ALP activity was normalized from the total protein content and total protein concentrations were determined using the micro bicinchoninic acid method (BCA, Sigma, USA) according to the instructions of the manufacturer. The concentration of each protein was calibrated using a standard curve according to the instructions of the manufacturer. Further analysis was then performed using the ELISA plate reader at 562 nm.

### 2.7 Initial cell spreading and cytoskeleton development

The messenger RNA (mRNA) expression of integrin-binding sialoprotein (IBSP), alkaline phosphatase (ALP), osteopontin (OPN), and osteocalcin (OCN) were quantitatively evaluated by real-time quantitative polymerase chain reaction (Q-PCR) (7500 fast real-time PCR System, Applied Biosystems, USA). After culturing for 7 days, the total RNA was extracted using the total RNA isolation kit (Geneaid, USA) according to the instructions of the manufacturer. Purified RNA was used to synthesize cDNA with MMLV reverse transcriptase (Invitrogen, USA). The resulting cDNA was used for the PCR reaction using Fast SYBR® Green Master Mix. The amplification profile involved denaturation at 95 °C for 20 s, followed by 40 cycles of 95 °C for 3 s, and 60 °C for 30 s following a

melting curve to check for amplicon specificity. Gene expression was normalized by glyceraldehyde 3-phosphate dehydrogenase (GAPDH) using the comparative cycle threshold (ddCt) method. The following primer sets were used to amplify each target sequence: GAPDH (forward: 5'-GGA GTA AGA AAC CCT GGA-3'; reverse: 5'-CTG GGA TGG AAA TTG TGA G-3'), IBSP (forward: 5'-CCG AGC TTA TGA GGA TGA ATA CA-3', reverse: 5'-GGT AGC CAG ATG ATA AGA CAG AAT-3'), ALP (forward: 5'-CTG CCT TGC CTG TAT CTG-3', reverse: 5'-GGT GCT TTG GGA ATC TGT-3'), OPN (forward: 5'-CTT TCA CTC CAA TCG TCC CTA-3'; reverse: 5'-GTC CTC ATC TGT GGC ATC A-3'), OCN (forward: 5'-TCG GCT TTG GCT GCT CTC-3'; reverse: 5'-CCT GCT GTG ACA TCC ATA CTT G-3').

### 2.8 Statistical analysis

At least five samples were obtained at each time point and the results are presented as the mean ± standard deviation (SD). One-way analysis of variance (ANOVA) and Duncan's post-hoc tests were performed for all assessments.

## 3. Results and discussion

### 3.1 Morphology and characteristics of poly(dopamine) film on MAO coatings

Figure 1 presents the surface morphologies of the specimens in this study. Compared to the untreated titanium substrate, the MAO process produced a much rougher surface with crater-like structures (Figs. 1c-f). The inset images were recorded at a tilt angle of 30° and clearly illustrate the three-dimensional structure of the coatings. All specimens presented coatings with uniform pore distribution and no obvious differences were observed among the specimens. The specimens were immersed directly in the dopamine solution, which resulted in the spontaneous formation of a self-polymerization layer on the specimens. As shown in Fig. 1b, specimen TiD was smoother than the Ti substrate with a covering of poly(dopamine). Compared with the pristine porous structure prior to dopamine treatment, a number of granular lumps comprising dopamine molecules can be seen on the surface (Figs. 1d and f, indicated by white arrow).

The topographies of the CaPD and SrCaPD specimens are similar to that of the CaP coating, suggesting that the poly(dopamine) formed an ultra-thin layer with little to no effect on the three-dimensional structure beneath. These results are consistent with several previous studies that reported the homogeneous coating of poly(dopamine) across the surface.[20, 22, 23] Under alkaline conditions, dopamine molecules are believed to undergo adsorption and self-polymerization simultaneously, which involves the oxidation of catechol to quinone, which then react with amines and other catechols/quinones to form an adherent polymer.[24] As a result, dopamine may provide strong covalent as well as noncovalent interactions with a variety of substrates without noticeably altering the topography.

**Figure 1.** Surface micrographs of specimens without and with added dopamine: (a) Ti; (b) TiD; (c) CaP; (d) CaPD; (e) SrCaP; (f) SrCaPD. The insets in (d)-(g) are highly magnified images obtained at a tilt of 30°. White arrows indicate granular lumps which comprising dopamine molecules.

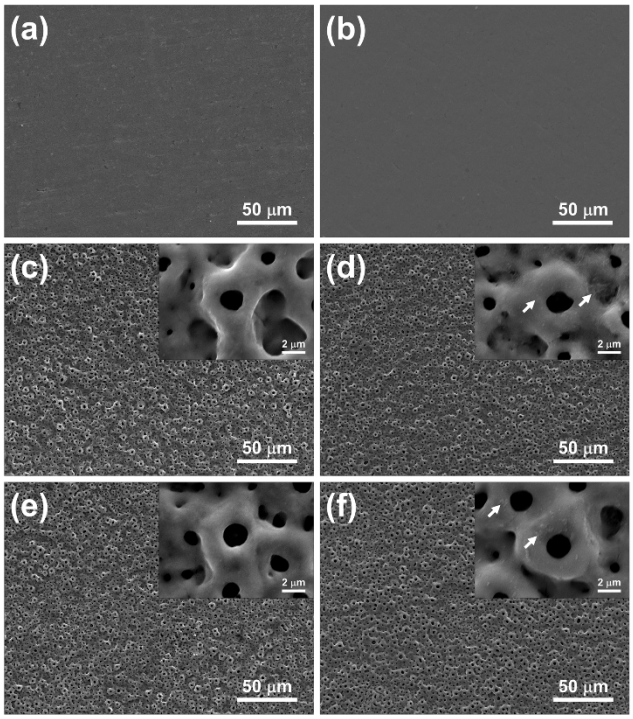


The surface hydrophilicity of biomaterials has been shown to be an important factor influencing cell responses.[25] In this study we used static water contact angle to evaluate the wettability of the specimens (Fig. 2). The static contact angle of droplets on as-polished titanium was 52.9° ± 5.6°. Following the MAO process, the water contact angle was approximately 10°, due to the hydrophilic nature of the coating. After being coated with poly(dopamine), the two MAO coatings differed only slightly, with an increase in contact angle of approximately 15°.

The MAO process with dopamine modification resulted in a surface with relatively hydrophilic properties. The hydrophilic nature of titanium surfaces has been shown to enhance protein adsorption, and thus promote the proliferation and differentiation of osteoblastic cells, and ultimately the strength of bone–implant integration.[26] In our previous study, the accumulation of adsorbed serum protein corresponded to an increase in DOPA content.[21] It is reasonable to speculate that a poly(dopamine) layer could be used to interconnect serum proteins and modulate cell attachment.[27]

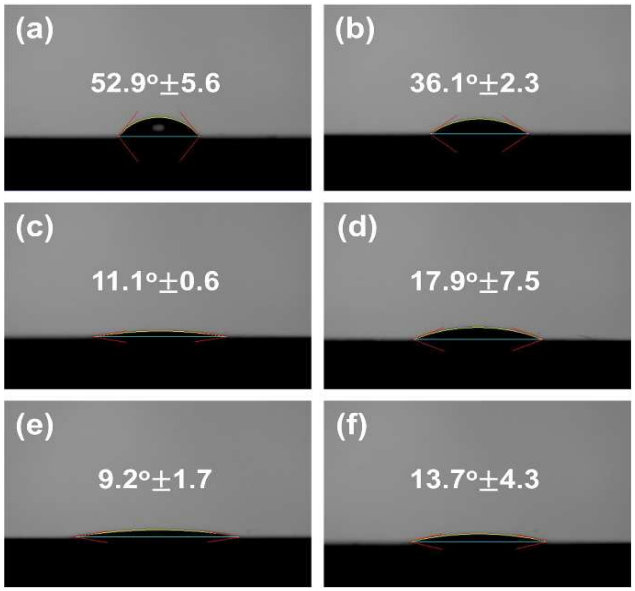


**Figure 2.** Water contact angle of all specimens in the study: (a) Ti; (b) TiD; (c) CaP; (d) CaPD; (e) SrCaP; (f) SrCaPD.

XPS analysis was used to investigate the surface chemistry in order to confirm the effectiveness of the coating process. Figure 3a (left) shows the XPS spectra of Ti, CaP, and SrCaP specimens, respectively. The survey spectra of the CaP specimen reveals peaks associated with Ti2p, O1s, C1s, Ca2p, and P2s. The addition of strontium to the electrolyte during MAO resulted in peaks associated with the presence of Sr3p1/2 and Sr3p3/2, confirming the incorporation of strontium into the oxide layer (Fig. 3b).

To ensure that the control group had the same ion release characteristics as the test samples, CaP and SrCaP specimens were also immersed in the Tris-HCl solution without dopamine. Our results suggest that differences in the strontium content could be attributed to the thickness of the poly(dopamine) coating. Following the coating process, we observed a nitrogen signal from the amino groups of dopamine molecules at 399.6 eV, as shown in Fig. 3c (right). The presence of such a nitrogen peak is an indication that the poly(dopamine) coating process was successful.

Table 2 presents a summary of the surface chemical composition obtained using XPS analysis. The nitrogen content for specimens TiD, CaPD, and SrCaPD was 7.9%, 7.9%, and 7.5%, respectively, indicating that the surface had indeed been coated with poly(dopamine) film, with only a negligible effect on the surface topography. Further, the composition of the substrate did not appear to have a significant effect on the amount of poly(dopamine) adhered to the substrate. The relative atomic concentration of C was 18.0% (TiD), 18.9% (CaPD), and 14.7 % (SrCaPD). After the specimens were coated with a poly(dopamine) film, the relative atomic concentrations of C increased to 68.4% (TiD), 68.3% (CaPD), and 66.7% (SrCaPD). The dopamine molecule contains amide and benzyl functional groups; therefore, the N1s and C1s signals in the XPS spectra can be attributed to the poly(dopamine) film on the MAO coatings. This also explains why the CaPD and SrCaPD specimens presented increased N/C ratios. The N/C ratios of the three specimens were close to the theoretical values of the dopamine molecule (0.125).[17] Analysis of surface chemical composition suggests that the strontium was incorporated within the coatings and that a film of poly(dopamine) had been successfully attached to the specimens.

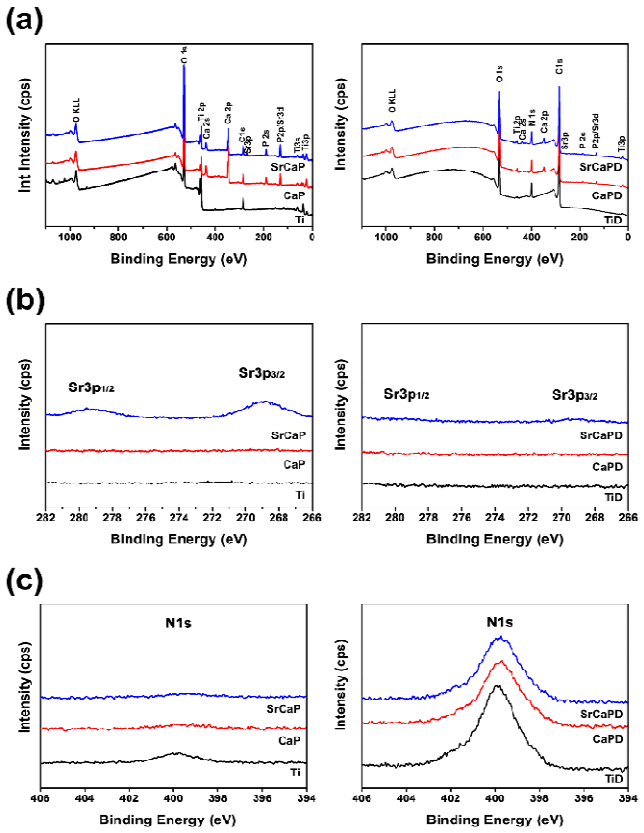


**Figure 3.** (a) Broad-range XPS spectra of specimens; (b) high resolution Sr3p spectra of specimens; (c) high resolution N1s spectra of specimens

### 3.2 Cell morphologies and cytoskeleton on poly(dopamine) film over MAO coatings

Understanding how osteoblasts interact with artificial materials is of crucial importance. The behaviour of osteoblast cells on the six specimens in this study was systematically examined in terms of initial cell spreading, cytoskeletal organization, proliferation, ALP activity, and bone-related gene expression. Cytoskeletal reorganization is particularly important in cell attachment, proliferation, and differentiation, all of which are essential to the initial success of an implant.[28, 29] In this study, we seeded MC3T3-E1 cells on each specimens to examine the cell-material interactions, using a fluorescence microscope was used to provide an accurate indication of cell spreading and cytoskeletal reorganization.

**Table 2.** Surface element composition of MAO coatings, as determined by XPS

| Specimen | Atomic % | | | | | | | |
|---|---|---|---|---|---|---|---|---|
| | Ti2p | O1s | C1s | Ca2p | P2p | Sr3p | N1s | N/C |
| Ti | 16.3 | 56.2 | 27.6 | -- | -- | -- | -- | -- |
| TiD | 0.3 | 17.7 | 74.1 | -- | -- | -- | 7.9 | 0.11 |
| CaP | 4.4 | 51.4 | 18.0 | 14.1 | 12.1 | -- | -- | -- |
| CaPD | 0.6 | 20.0 | 68.4 | 1.6 | 1.5 | -- | 7.9 | 0.12 |
| SrCaP | 6.4 | 46.8 | 18.0 | 9.6 | 16.0 | 1.6 | -- | -- |
| SrCaPD | 0.6 | 20.2 | 68.3 | 1.3 | 2.0 | 0.1 | 7.6 | 0.11 |

MC3T3-E1 showed the characteristic pattern of complex focal adhesion with a dense phalloidin stained f-actin (green) surrounded by vinculin (red) staining at the leading edge of cells (Figs. 4 and 5). Figure 4 presents the morphologies of the cells grown on specimens for 3 h. Clearly, the MC3T3-E1 cells rapidly attached to the surface of all of the specimens; however, the attachment rates varied according to the features of the specimens. The MC3T3-E1 cells appeared to have spread well and formed focal adhesion to the flat Ti specimen. Cells cultured on TiD specimens showed spreading over a greater area than on the Ti specimens (Figs. 4a and b). Cells cultured on the CaP specimen presented no evidence of stress fibers, which is an indication of limited interaction with the substrate (Fig. 4c).

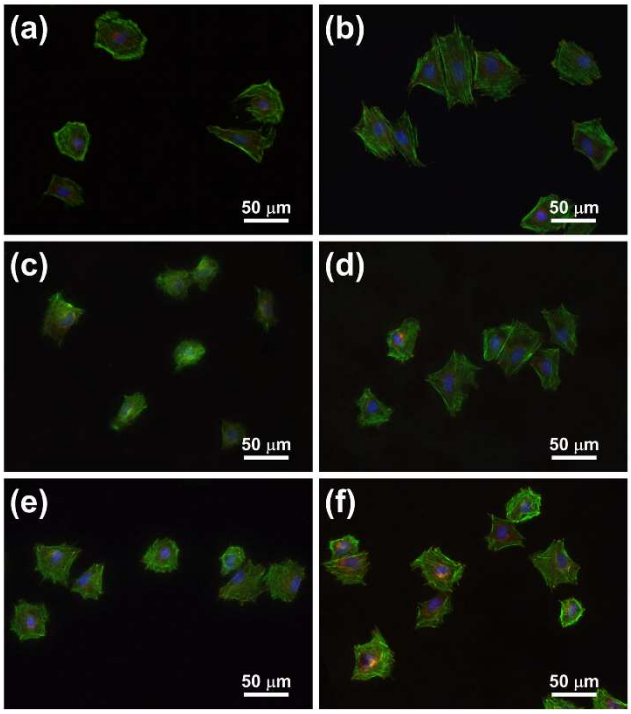


**Figure 4.** Fluorescence images of MC3T3-E1 cells cultured on various specimens after 3h of incubation: (a) Ti; (b) TiD; (c) CaP; (d) CaPD; (e) SrCaP; (f) SrCaPD. F-actin (green) was stained with Alexa Flour 488 phalloidin, vinculin (red) was stained with Alexa Fluor 594, and the nucleus (blue) was stained with DAPI.

Cells covered a greater area of the SrCaP specimens than the CaP specimens (Fig. 4e). The presence of poly(dopamine) film appears to have promoted cell attachment on the CaPD and SrCaPD specimens, resulting in long extensions of cytoplasmic membranes, which spread out to assume a fully flattened shape (Figs. 4d and f). The shape and morphology of the cells indicated that poly(dopamine) film promoted the attachment and spreading of osteoblastic cells.

Following an incubation period of 24 h, we observed the expansion of actin filaments in cell cultures grown on poly(dopamine) modified specimens. The filaments exhibited a flattened polygonal morphology spread over a wider area (Figs. 5b, d, and f). Compared to cells cultured on unmodified specimens, those cultured on poly(dopamine)-coated surfaces presented well-stretched actin bundles and highly organized actin stress fibers, which is a clear indication of strong cell adhesion at the interface. The poly(dopamine) film was also found to induce the extension of lamellipodia on SrCaPD specimens (Fig. 5f). A number of previous studies have reported that the roughness of substrates strongly influences MC3T3-E1 cell adhesion; however, in those studies, rough surfaces resulted in less proliferation and adhesion than did smooth surfaces.30, 31 This difference in surface topography may explain why the cells cultured on Ti specimens exhibited attachment characteristics superior to those cultured on CaP specimens. In contrast, cells cultured on CaPD and SrCaPD presented expansion characteristics far exceeding those on the CaP and SrCaP specimens, which suggests that the poly(dopamine) film had improved MC3T3-E1 cell adhesion, particularly on samples with a more porous structure.

Controlling cell adhesion is crucial in this type of organic-inorganic system, because adhesion provides a physical link to the environment and influences all of the major cell fate decisions, including cellular signal transduction, differentiation, and gene expression.[32] A higher density of actin stress fibres in the cytoskeleton of a cell indicates a firmer, stronger link between the cells and substrate. This, in turn, indicates that a given biomaterial is suitable for cell attachment and the preservation of biological functions.[33] As previously reported, bioactive functional groups, such as the hydroxyl and amine groups that form dopamine, may be beneficial to the process of cell attachment. In this study, dopamine appears to have played a

major role in this process. It appears that combining dopamine and strontium ions significantly enhances initial cell attachment, thereby strengthening the link between cells and MAO coatings.

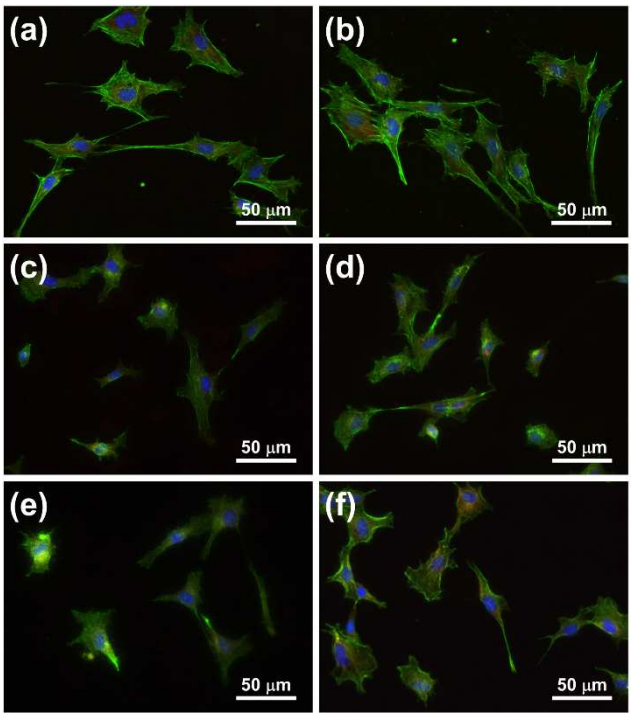


**Figure 5.** Fluorescence images of MC3T3-E1 cells cultured on various specimens after 24 h of incubation: (a) Ti; (b) TiD; (c) CaP; (d) CaPD; (e) SrCaP; (f) SrCaPD. F-actin (green) was stained with Alexa Flour 488 phalloidin, vinculin (red) was stained with Alexa Fluor 594, and the nucleus (blue) was stained with DAPI.

### 3.3 Cell proliferation and differentiation on MAO coatings further coated with strontium and dopamine

Figure 6 presents the number of MC3T3-E1 cells on the surface of each specimen after culturing for 1, 3, and 7 days, respectively. All of the specimens presented an increase in the number of cells, indicating that the MC3T3-E1 cells proliferated continuously throughout the 7 days. After days 1, 3, and 7, the number of cells on the TiD, CaPD and SrCaPD specimens was significantly higher than on the unmodified specimens. Nonetheless, after 7 days, the number of cells on pure titanium was significantly higher than on specimens of CaP and SrCaP. The number of cells on the CaPD and SrCaPD specimens exceeded the numbers observed on any samples without poly(dopamine) modification.

ALP is a marker of early stage osteoblast differentiation, which undergoes a sequence of processes eventually resulting in the formation of bone. Figure 7 presents the ALP activity of MC3T3-E1 cell on the surface of each specimen over the 7-day incubation period. Previously, the presence of strontium ions was reported to be advantageous to cell differentiation.[14] In this study, the ALP activity of MC3T3-E1 cells on SrCaP and SrCaPD specimens was significantly more pronounced than that observed on CaP and CaPD specimens, indicating that the incorporation of strontium may improve the initiation of osteogenic differentiation in MC3T3-E1 cells.

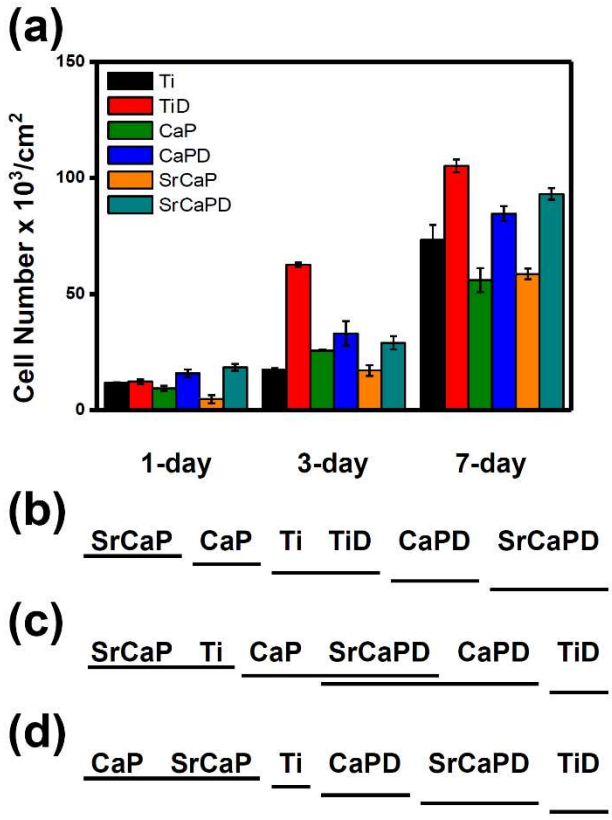


**Figure 6.** MTT cell proliferation assay results for MC3T3-E1 cells after culturing on various specimens for 1, 3, and 7 days: (a) Measurements from the MTT cell proliferation assay, (b) Duncan grouping of the 1-day MTT assay, (c) Duncan grouping of the 3-day MTT assay, and (d) Duncan grouping of the 7-day MTT assay

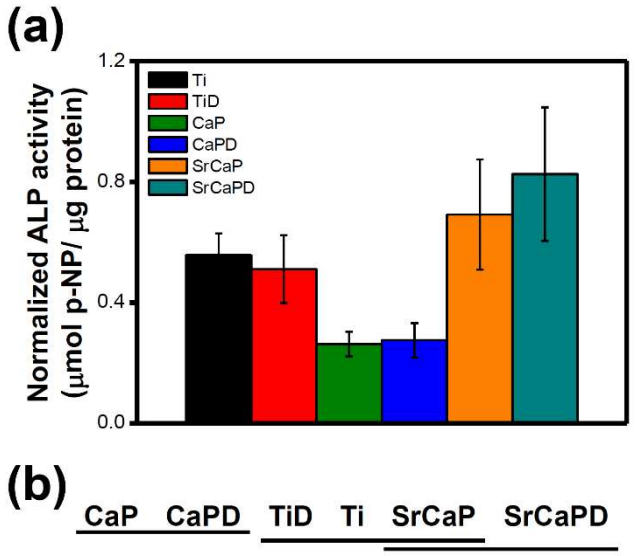


**Figure 7.** (a) Results of ALP activity for MC3T3-E1 cells cultured on various specimens. The values represent average ± standard deviation (n = 5). (b) Duncan grouping of ALP activity.

To quantify the differentiation of the MC3T3-E1 cells, we measured the expression of osteogenic marker genes including integrin-binding sialoprotein (IBSP), alkaline phosphatase (ALP), osteopontin (OPN) and osteocalcin (OCN) using quantitative reverse transcription PCR. Our results show that the SrCaP and SrCaPD specimens promoted bone-related gene expression, such as IBSP, ALP, OPN, and OCN (Fig. 8). Strontium-based artificial materials, including strontium-substituted hydroxyapatite cement and bioactive glasses, have been attracting interest due to the appearance of a link between strontium and the stimulation of osteoblast differentiation and the inhibition of osteoclast formation and resorption *in vitro*. The results indicate that strontium enhances cell differentiation, as evidenced by the up-regulation of bone-related mRNA.[14]

The surface chemistry and topography of materials can influence the response of osteoblastic cells. Surfaces with a moderately rough microstructure, such as MAO, have been shown to enhance the maintenance of implant stability.[34, 35] Several studies have demonstrated that strontium can increase the quality of bone structure and promote bone ingrowth, thereby accelerating implant osseointegration.[36, 37] The SrCaPD coating altered the topography as well as the surface chemistry. The resulting increase in cell adhesion and ALP activity are in good agreement with previous reports. Our results suggest that dopamine and strontium both play important roles in stimulating the proliferation and differentiation of MC3T3-E1 cells. These effects are most pronounced on the SrCaPD sample with the best cell attachment, proliferation, and differentiation of MC3T3-E1 cells.

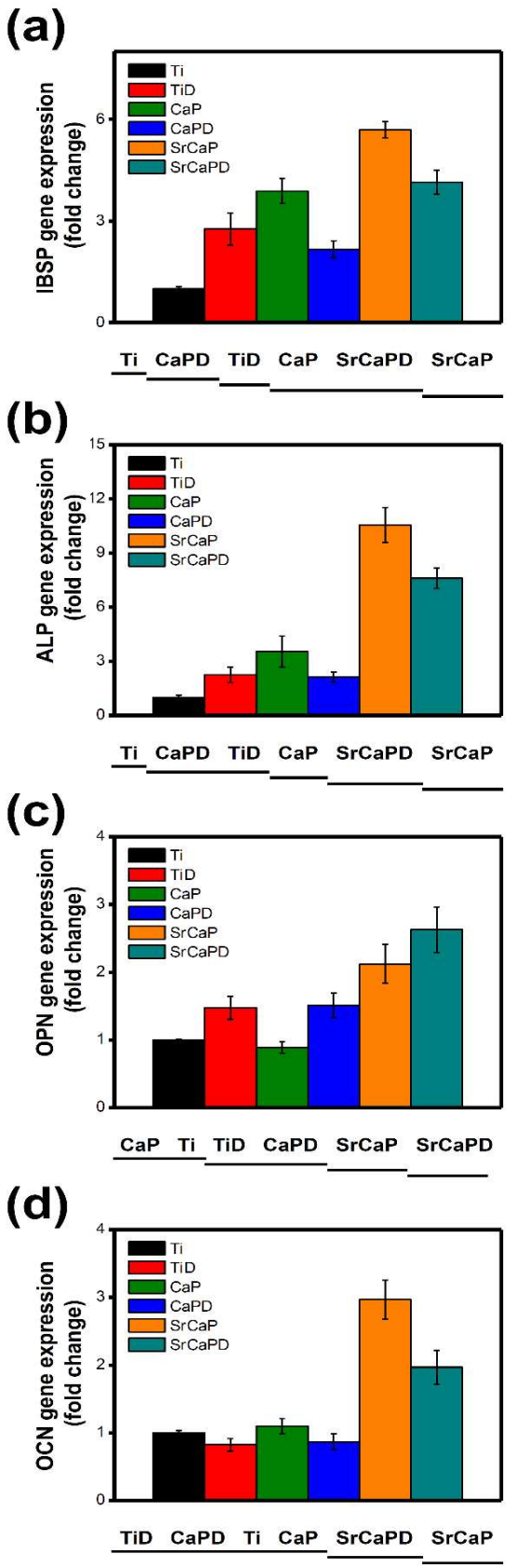


**Figure 8.** Bone-related gene expression of osteoblast cells cultured on various specimens in terms of (a) IBSP, (b) ALP, (c) OPN, and (d) OCN.

## 4. Conclusions

This study developed an innovative coating for titanium surfaces combining MAO with bio-inspired surface modification. The proposed method creates an excellent three-dimensional structure, the topography of which is in no way jeopardized by the application of a bioactive layer to promote cell attachment and cytoskeletal development. Moreover, the incorporation of strontium-ions in the MAO coating was shown to greatly induce osteoblasts cell differentiation. This novel dual-setting material provides many of the benefits anticipated in the next generation of bio-modified implants.

## Acknowledgements

This work was financially supported by the National Science Council, Taiwan, under grant NSC 100-2221-E-006-263.

## Notes and references

[a] Department of Materials Science and Engineering, National Cheng Kung University, Tainan, Taiwan
[b] Institute of Oral Medicine, National Cheng Kung University, Tainan, Taiwan; Email: tmlee@mail.ncku.edu.tw Tel.: +886-6-2353535 ext. 5972, Fax: +886-6-2095845
[c] Department of Orthopedics, National Cheng Kung University, Tainan, Taiwan

1 L. Zhu, X. Ye, G. Tang, N. Zhao, Y. Gong, Y. Zhao, J. Zhao and X. Zhang, *J. Biomed. Mater. Res., Part A*, 2006, **78A**, 515-522.
2. X. Zhao, G. Wang, H. Zheng, Z. Lu, X. Zhong, X. Cheng and H. Zreiqat, *ACS Appl. Mater. Interfaces*, 2013, **5**, 8203-8209.
3. K. P. Ananth, S. Suganya, D. Mangalaraj, J. M. Ferreira and A. Balamurugan, *Mater. Sci. Eng., C*, 2013, **33**, 4160-4166.
4. E. R. Urquia Edreira, J. G. C. Wolke, A. A. Aldosari, S. S. Al-Johany, S. Anil, J. A. Jansen and J. J. J. P. van den Beucken, *J. Biomed. Mater. Res., Part A*, 2014, DOI: 10.1002/jbm.a.35173.
5. C. W. Yang and T. S. Lui, *Mater. Trans.*, 2007, **48**, 211-218.
6. L. H. Li, Y. M. Kong, H. W. Kim, Y. W. Kim, H. E. Kim, S. J. Heo and J. Y. Koak, *Biomaterials*, 2004, **25**, 2867-2875.
7. M. Degidi, D. Nardi and A. Piattelli, *Clin Implant Dent Relat Res*, 2012, **14**, 828-838.
8. C. Ma, A. Nagai, Y. Yamazaki, T. Toyama, Y. Tsutsumi, T. Hanawa, W. Wang and K. Yamashita, *Acta Biomater.*, 2012, **8**, 860-865.
9. Y. Han, D. Chen, J. Sun, Y. Zhang and K. Xu, *Acta Biomater.*, 2008, **4**, 1518-1529.
10. W. H. Song, H. S. Ryu and S. H. Hong, *J. Biomed. Mater. Res., Part A*, 2009, **88A**, 246-254.
11. Y. T. Liu, K. C. Kung, T. M. Lee and T. S. Lui, *J. Alloys Compd.*, 2013, **581**, 459-467.
12. G. X. Ni, W. W. Lu, K. Y. Chiu, Z. Y. Li, D. Y. T. Fong and K. D. K. Luk, *J. Biomed. Mater. Res., Part B*, 2006, **77B**, 409-415.
13. Y. W. Li, J. C. Y. Leong, W. W. Lu, K. D. K. Luk, K. M. C. Cheung, K. Y. Chiu and S. P. Chow, *J. Biomed. Mater. Res.*, 2000, **52**, 164-170.
14. C. Capuccini, P. Torricelli, F. Sima, E. Boanini, C. Ristoscu, B. Bracci, G. Socol, M. Fini, I. N. Mihailescu and A. Bigi, *Acta Biomater.*, 2008, **4**, 1885-1893.
15. Y. Zhang, L. Wei, J. Chang, R. J. Miron, B. Shi, S. Yi and C. Wu, *J. Mater. Chem. B*, 2013, **1**, 5711-5722.
16. K. C. Kung, T. M. Lee, J. L. Chen and T. S. Lui, *Surf. Coat. Technol.*, 2010, **205**, 1714-1722.
17. H. Lee, S. M. Dellatore, W. M. Miller and P. B. Messersmith, *Science*, 2007, **318**, 426-430.
18. S. Saidin, P. Chevallier, M. R. Abdul Kadir, H. Hermawan and D. Mantovani, *Mater. Sci. Eng., C*, 2013, **33**, 4715-4724.
19. T. Liu, Z. Zeng, Y. Liu, J. Wang, M. F. Maitz, Y. Wang, S. Liu, J. Chen and N. Huang, *ACS Appl. Mater. Interfaces*, 2014, DOI: 10.1021/am5015309.
20. C. Y. Chien, T. Y. Liu, W. H. Kuo, M. J. Wang and W. B. Tsai, *J. Biomed. Mater. Res., Part A*, 2013, **101A**, 740-747.
21. Y. T. Liu, T. M. Lee and T. S. Lui, *Colloids Surf., B*, 2013, **106**, 37-45.
22. N. G. Rim, S. J. Kim, Y. M. Shin, I. Jun, D. W. Lim, J. H. Park and H. Shin, *Colloids Surf., B*, 2012, **91**, 189-197.
23. W. Wang, R. Li, M. Tian, L. Liu, H. Zou, X. Zhao and L. Zhang, *ACS Appl. Mater. Interfaces*, 2013, **5**, 2062-2069.
24. R. A. Zangmeister, T. A. Morris and M. J. Tarlov, *Langmuir*, 2013, **29**, 8619-8628.
25. P. Thevenot, W. Hu and L. Tang, *Curr. Top. Med. Chem*., 2008, **8**, 270-280.
26. J. H. Park, C. E. Wasilewski, N. Almodovar, R. Olivares-Navarrete, B. D. Boyan, R. Tannenbaum and Z. Schwartz, *Biomaterials*, 2012, **33**, 7386-7393.
27. Y. Ding, Z. Yang, C. W. C. Bi, M. Yang, J. Zhang, S. L. Xu, X. Lu, N. Huang, P. Huang and Y. Leng, *J. Mater. Chem. B*, 2014, DOI: 10.1039/C4TB00386A.
28. M. Ghibaudo, A. Saez, L. Trichet, A. Xayaphoummine, J. Browaeys, P. Silberzan, A. Buguin and B. Ladoux, *Soft Matter*, 2008, **4**, 1836-1843.
29. K. Anselme, *Biomaterials*, 2000, **21**, 667-681.
30. K. Anselme, P. Linez, M. Bigerelle, D. Le Maguer, A. Le Maguer, P. Hardouin, H. F. Hildebrand, A. Iost and J. M. Leroy, *Biomaterials*, 2000, **21**, 1567-1577.
31. K. Anselme, M. Bigerelle, B. Noel, E. Dufresne, D. Judas, A. Iost and P. Hardouin, *J. Biomed. Mater. Res.*, 2000, **49**, 155-166.
32. O. Guillame-Gentil, O. Semenov, A. S. Roca, T. Groth, R. Zahn, J. Vörös and M. Zenobi-Wong, *Adv. Mater.*, 2010, **22**, 5443-5462.
33. W. Thein-Han and H. H. K. Xu, *Tissue Eng., Part A*, 2011, **17**, 2943-2954.
34. W. Zechner, S. Tangl, G. Fürst, G. Tepper, U. Thams, G. Mailath and G. Watzek, *Clin Oral Implants Res*, 2003, **14**, 150-157.
35. A. Rocci, M. Martignoni, P. M. Burgos, J. Gottlow and L. Sennerby, *Clin Implant Dent Relat Res*, 2003, **5**, 88-98.
36. O. Z. Andersen, V. Offermanns, M. Sillassen, K. P. Almtoft, I. H. Andersen, S. Sørensen, C. S. Jeppesen, D. C. E. Kraft, J. Bøttiger, M. Rasse, F. Kloss and M. Foss, *Biomaterials*, 2013, **34**, 5883-5890.
37. L. Maïmoun, T. C. Brennan, I. Badoud, V. Dubois-Ferriere, R. Rizzoli and P. Ammann, *Bone*, 2010, **46**, 1436-1441.

# Graphic abstract